

## *E. coli* Multidrug Transporter MdfA Is a Monomer<sup>†</sup>

Nadejda Sigal,<sup>‡,||</sup> Oded Lewinson,<sup>‡,||,⊥</sup> Sharon G. Wolf,<sup>§</sup> and Eitan Bibi<sup>\*‡</sup>

Department of Biological Chemistry, Weizmann Institute of Science, Rehovot 76100, Israel, and Electron Microscopy Unit of the Weizmann Institute, Weizmann Institute of Science, Rehovot 76100, Israel

Received November 21, 2006; Revised Manuscript Received February 24, 2007

**ABSTRACT:** MdfA is a 410-residue-long secondary multidrug transporter from *E. coli*. Cells expressing MdfA from a multicopy plasmid exhibit resistance against a diverse group of toxic compounds, including neutral and cationic ones, because of active multidrug export. As a prerequisite for high-resolution structural studies and a better understanding of the mechanism of substrate recognition and translocation by MdfA, we investigated its biochemical properties and overall structural characteristics. To this end, we purified the  $\beta$ -dodecyl maltopyranoside (DDM)-solubilized protein using a 6-His tag and metal affinity chromatography, and size exclusion chromatography (SE-HPLC). Purified MdfA was analyzed for its DDM and phospholipid (PL) content, and tetraphenylphosphonium (TPP<sup>+</sup>)-binding activity. The results are consistent with MdfA being an active monomer in DDM solution. Furthermore, an investigation of two-dimensional crystals by electron crystallography and 3D reconstruction lent support to the notion that MdfA may also be monomeric in reconstituted proteoliposomes.

The simultaneous emergence of resistance in eukaryotic and prokaryotic cells to many unrelated cytotoxic agents is termed multidrug resistance (Mdr<sup>1</sup>). A major form of multidrug resistance is caused by Mdr transporters that remove multiple drugs from the cell cytoplasm or cytoplasmic membrane to the external medium (1, 2). These transporters are able to extrude a large variety of chemically unrelated, usually lipophilic compounds, which are positively or negatively charged under physiological conditions, as well as neutral and zwitterionic compounds (3–6). Therefore, in addition to their potential clinical importance (7), Mdr transporters pose intriguing questions regarding substrate recognition, energy coupling, and transport mechanism. On the basis of bioenergetic and structural criteria, Mdr transporters belong to at least five different families of transport proteins driven either by ATP (ABC Mdr transporters) or by ion electrochemical gradients (Mdr transporters of the MFS, RND, MATE, and DMT superfamilies) (8, 9).

MdfA is an *Escherichia coli* Mdr transporter of the major facilitator superfamily (MFS) (10, 11), which serves as a model in our studies of secondary Mdr transport (3, 12, 13). Very close homologues of MdfA were identified in pathogenic bacteria: *Shigella flexneri* (99% homology) (14),

*Salmonella enterica* serovar Typhi (90% homology) (15), and *Yersinia pestis* (73% homology) (16). MdfA is a multidrug/proton antiporter with a remarkably broad substrate specificity profile (3, 17, 18). In addition to its function as an Mdr transporter, recent studies revealed that MdfA plays a physiological role in alkaline pH homeostasis, possibly through its K<sup>+</sup>/proton antiporter activity (19). Limited structural information about MdfA has been revealed through hydrophobicity profiling (3), gene fusion analyses (20, 21), several cysteine accessibility experiments (22, 23), and homology modeling (24). According to the emerging model, MdfA is a typical MFS-related 12 transmembrane helix (TM) protein with a large and complex multidrug recognition pocket. However, direct structural information is required for a better understanding of the molecular mechanism by which MdfA recognizes and transports multiple dissimilar substrates. As a critical step toward high-resolution structural studies of MdfA, we have characterized its biochemical properties in detergent solution. These studies revealed that every solubilized MdfA molecule is accompanied by PLs and detergent molecules, with a stoichiometry that is dependent on the detergent concentration used during the purification protocol. The results of the biochemical studies, in combination with a low-resolution 3D map of the protein derived from electron microscopy analysis of 2D crystals, strongly suggest that MdfA is a monomer in detergent solution and possibly also in proteoliposomes.

### EXPERIMENTAL PROCEDURES

**Preparation of MdfA Membranes.** *E. coli* UTL2mdfA::kan (21) harboring plasmid pUC18/Para/mdfA<sub>6HIS</sub> (25) were grown at 37 °C in LB medium supplemented with ampicillin (200  $\mu$ g/mL) and kanamycin (30  $\mu$ g/mL). Overnight cultures were diluted to 0.07 OD<sub>600</sub> units, grown to 1.0 OD<sub>600</sub> units, and cooled down to 25 °C. The culture was then induced with 0.2% arabinose for 2 h. A typical 10-L culture yielded

<sup>†</sup> This work was supported by a grant from the Israel Cancer Research Foundation (ICRF) and the Israel Science Foundation (ISF).

\* Corresponding author. Tel: +972-8-9343464. Fax: +972-8-9344118. E-mail: e.bibi@weizmann.ac.il.

<sup>‡</sup> Department of Biological Chemistry.

<sup>§</sup> Electron Microscopy Unit of the Weizmann Institute.

<sup>||</sup> These authors contributed equally to this work.

<sup>⊥</sup> Current address: Division of Chemistry and Chemical Engineering, California Institute of Technology, 1200 E. California Blvd., Pasadena, CA 91125.

<sup>1</sup> Abbreviations: LB, Luria–Bertani medium; Mdr, multidrug resistance; KPi, potassium phosphate buffer; TPP<sup>+</sup>, tetraphenylphosphonium; SE-HPLC, size exclusion high performance liquid chromatography; MFS, major facilitator superfamily; DDM,  $\beta$ -dodecyl maltopyranoside; PL, phospholipid; TM, transmembrane helix.

~15 g (wet weight) of cells. Cell pellets were washed once in 150 mL of 50 mM KPi (pH 7.3) supplemented with 2 mM MgSO<sub>4</sub> and 14 mM  $\beta$ -mercaptoethanol and collected by centrifugation (15 min, 5,000g). Next, the cells were suspended in 90 mL of the same buffer containing 10  $\mu$ g/mL DNase and 0.5 mM pefablock and passed three times through a liquidizer (Emulsiflex-C5, Avestin) (10,000 psi) for disruption. Cell debris was removed by centrifugation (30 min, 8,000g), and the membranes were collected by ultracentrifugation (1 h, 250,000g). The membranes were homogenized in 27 mL of urea buffer (20 mM Tris-HCl at pH 8, 0.5 M NaCl, 5 M urea, 10% glycerol, 28 mM  $\beta$ -mercaptoethanol, and 0.5 mM pefablock), incubated by tilting for 30 min at 4 °C, and collected by ultracentrifugation (3 h, 250,000g). The membranes were washed with 27 mL of buffer A (20 mM Tris-HCl at pH 8, 0.5 M NaCl, 10% glycerol, and 3.5 mM  $\beta$ -mercaptoethanol). Finally, the membranes were suspended by homogenization in 14 mL of buffer A, and aliquots of 3.5 mL were snap-frozen in liquid nitrogen and stored at -80 °C.

**Membrane Solubilization and MdfA Purification.** For solubilization, an aliquot (3.5 mL, see above) of membranes was thawed quickly at 37 °C and then supplemented with 7.5 mL of buffer A. The membranes were homogenized and solubilized by 1.7 mL of 10%  $\beta$ -dodecyl maltopyranoside (DDM) (final concentration 1.2%) added in four aliquots (0.425 mL) separated by intensive homogenization. The mixture was then agitated for 30 min at 4 °C. Insoluble material was discarded by ultracentrifugation (30 min, 100,000g), and the soluble fraction was mixed with buffer A-equilibrated Talon beads (Clontech) (1.3 mL). Next, the mixture was agitated for 3 h at 4 °C, and the suspension was poured into a column. The column was then washed (2  $\times$  7.5 mL of buffer A without glycerol, supplemented by 5 mM imidazole and either 0.01% or 0.1% DDM). MdfA was eluted in 4 mL of the elution buffer (20 mM Tris-HCl at pH 7.2, 0.5 M NaCl, 100 mM imidazole, 0.01% or 0.1% DDM, and 3.5 mM  $\beta$ -mercaptoethanol) and dialyzed overnight against buffer B (20 mM Tris-HCl at pH 7.2, 0.12 M NaCl, and 0.01% or 0.1% DDM) at 4 °C. Protein (approximately 0.25 mg in 0.5 mL) was analyzed by SE-HPLC using a Superdex200 10/300 GL column (Amersham Biosciences) and ice-cold buffer B containing either 0.01% or 0.1% DDM at a flow rate of 0.3 mL/min.

**DDM Assay.** The concentration of DDM was determined as previously described (26). Briefly, a 60  $\mu$ L-sample was mixed with 0.3 mL of 5% (w/v) phenol and then with 0.72 mL of concentrated sulfuric acid, followed by immediate vortexing. After cooling to room temperature (30 min), the OD<sub>490</sub> of each sample was measured. Each standard solution was measured in duplicate and the chromatography fractions in triplicate. The amount of MdfA-associated DDM was determined from the amount of DDM in the protein sample less that in a buffer without protein.

**PLs Assay.** The concentration of PLs was determined using a modified colorimetric assay for inorganic phosphate. An acid solution was prepared by mixing 40 mL of concentrated sulfuric acid and 20 mL of perchloric acid with 60 mg of vanadium (IV) oxide for 3–4 h. A powder mix containing 15 g of sodium metabisulfide, 0.25 g of 4-amino-3-hydroxy-1-naphthalenesulfonic acid, and 0.5 g of sodium sulfite was prepared and stored in the dark. Freshly prepared solution

A (50 mL) was obtained by dissolving 0.31 g of the powder mix and 0.1 g of ammonium molybdate in double distilled water. For the determination of PL concentration, 0.125 mL of the acid solution was added in a glass tube to each sample: 0.2 mL containing 5–100 nmol of phosphate, as K<sub>2</sub>HPO<sub>4</sub> for calibration, or 0.1 mL 2 $\times$ -distilled water + 0.1 mL of each of the test samples. The tubes were heated (directly on a flame) until an orange color appeared. Solution A (2.5 mL) was then added, and the samples were heated to 100 °C for 8 min. After cooling to room temperature, OD<sub>820</sub> was measured. Each calibration sample was determined in duplicate and the test samples in triplicate.

**Protein Assay.** The concentration of MdfA was initially directly analyzed by amino acid analysis (Chemical Services Unit of the Weizmann Institute of Science). For this purpose, MdfA samples of 50  $\mu$ L were dialyzed overnight against 80 mL of 2 $\times$ -distilled water in order to decrease solute concentrations. The amino acid analysis of each sample was performed in triplicate. The amino acid analysis was then utilized to produce a conversion factor (1.1) that enabled the determination of MdfA concentration by the BCA protein assay kit (Pierce). In addition, we were able to determine the absorbance coefficient for MdfA (1 mg/mL ~ 2.1 OD<sub>280</sub> units).

**TPP<sup>+</sup> Binding Assay.** Binding assays were performed essentially as described (25) with the following modifications. Purified protein (0.1–0.3 mg) was mixed with Ni-NTA beads (300  $\mu$ L) in 5 mL of buffer C (20 mM Tris-HCl at pH 8, 0.5 M NaCl, and the indicated DDM concentration) and gently agitated for 30 min at 4 °C. The unbound material (supernatant) was discarded by brief centrifugation (700g for 2 min). The beads were then washed with buffer C and resuspended in 3.2 mL of buffer D (20 mM Tris-HCl at pH 7, 0.5 M NaCl, and the indicated DDM concentration), divided into 200  $\mu$ L aliquots, which were incubated (10 min, 4 °C) with 50 nM of [<sup>3</sup>H]TPP<sup>+</sup> (2 Ci/mmol) and increasing concentrations of unlabeled TPP<sup>+</sup> (0.6–50  $\mu$ M). An aliquot of 180  $\mu$ L of the resin-MdfA-[<sup>3</sup>H] TPP<sup>+</sup> mixture was then transferred to a Promega Wizard minicolumn on top of a microfuge tube and centrifuged at 10,000g for 20 s. Unbound (flow-through) material was discarded, and the resin was re-suspended in 100  $\mu$ L of buffer D containing 350 mM imidazole. The radioactivity of this suspension was measured by liquid scintillation. The amount of [<sup>3</sup>H]TPP<sup>+</sup> bound to the resin in the absence of MdfA was subtracted from all measurements.

**Two-Dimensional Crystallization and Sample Preparation.** For the formation of 2D crystals, a combination of methods was used (27–30). Essentially, a solution of purified MdfA (1 mg/mL) was mixed with detergent-solubilized *E. coli* polar lipids (Avanti polar lipids) (4 mg/mL in 1% DM) to the desired protein/lipid ratio in the range of 0.1–5. After 16 h of incubation at 4 °C, the sample was dialyzed for 10 days against a 2000-fold volume of the crystallization solution (20 mM NaOAc adjusted to the desired pH in the range of 6–9.5, 3 mM NaN<sub>3</sub>, 5 mM  $\beta$ -mercaptoethanol, and the desired salt concentration in the range of 0–500 mM) (see Results). Where indicated, 40 mg/mL Bio-beads (Biorad) were added to the dialysis buffer. Five microliters of a sample were then applied for 1 min to a glow-discharged carbon coated (~10 nm) copper 400-mesh grid, and the sample was stained for 45 s by applying 5  $\mu$ L of 1% uranyl acetate.

**Electron Microscopy.** Samples were scanned using an FEI T-12 electron microscope operating at an acceleration voltage of 120 kV. Images were recorded at room temperature using standard low-dose procedures, at a nominal magnification of 59,000 on Kodak SO163 film. Tilted images were collected from  $-45^\circ$  to  $+45^\circ$ , at intervals of  $15^\circ$ .

**Image Processing.** Micrographs were developed for 12 min in a Kodak D-19 full-strength developer and were evaluated using a homemade laser optical bench. Images showing ordered diffraction were digitized using a Creo Eversmart Supreme scanner at 2.2 Å per pixel. The best images were processed using the standard MRC package (31). Following correction for lattice distortions (unbending), images were corrected for the effects of the contrast transfer function (CTF). Using the image showing the highest order as a reference, a common phase origin was determined (and refined) for all the images to be merged. The final projection map was calculated from the merged amplitudes and phases of eight unbent and CTF corrected images.

**Three-Dimensional Reconstruction.** The projection data set was sequentially merged to the data of increasingly tilted images, employing iterative cycles for tilt geometry refinement. Curve fitting to the experimental structure factors was performed using the program LATLINE (32), and the 3D density map was produced using the CCP4 program suite.

## RESULTS

Previously, we utilized metal affinity techniques for the purification of MdfA tagged with six histidines at the C-terminus (MdfA<sub>6HIS</sub>) (17, 19, 25, 33). This purification protocol yielded functional MdfA in detergent solution, as shown by direct TPP<sup>+</sup>-binding assays. However, these studies revealed a stoichiometry of 0.6:1 (TPP<sup>+</sup>/MdfA), suggesting that either MdfA functions as a dimer or that a substantial fraction of the purified protein was inactive. In order to distinguish between these possibilities, MdfA was solubilized and purified under various conditions, its biochemical properties were characterized, and its overall structural features were studied by 2D crystallization and electron microscopy.

**Single Step Purification of MdfA.** DDM-solubilized membranes prepared from MdfA-overexpressing cells (25) were incubated with Talon cobalt resin and divided into two samples, which were washed and eluted in either 0.01% or 0.1% DDM as described in Experimental Procedures. Samples from each purification step were analyzed by SDS-PAGE (Figure 1), and the results show that MdfA is significantly overexpressed (Figure 1, lane 1), and approximately 30% can be solubilized by 1.2% DDM (Figure 1, lane 2). Furthermore, under the conditions used for binding to the Talon resin, only MdfA was found bound to the beads (Figure 1, compare lane 2 with lane 3). The single step purification protocol yielded highly purified MdfA, regardless of the DDM concentration used in the final steps (Figure 1, lanes 6 and 7). This preparation of MdfA, which is usually utilized in our functional and structural studies, was characterized further by SE-HPLC (Figure 1, lanes 8 and 9).

**Characterization of Purified MdfA by SE-HPLC.** The elution profiles of the two MdfA preparations through a Superdex200 column confirms that indeed the metal affinity purification yielded a highly pure and monodispersed protein

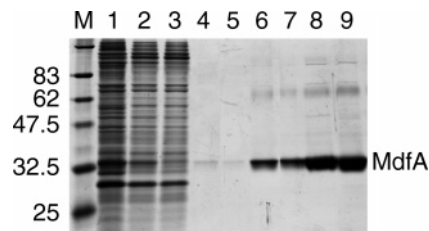


FIGURE 1: Purification of MdfA<sub>6HIS</sub> at different DDM concentrations. Samples withdrawn during the purification of MdfA were analyzed by SDS-PAGE and Coomassie blue staining. M denotes the molecular mass marker. Lane 1, total membrane proteins; lane 2, solubilized fraction; lane 3, Talon-unbound fraction; lane 4, 0.1% DDM column wash fraction; lane 5, 0.01% DDM column wash fraction; lane 6, 0.1% DDM elution fraction; lane 7, 0.01% DDM elution fraction; lane 8, concentrated ( $\times 10$ ) SE-HPLC fraction (in 0.1% DDM); and lane 9, concentrated ( $\times 10$ ) SE-HPLC fraction (in 0.01% DDM). Lanes 1–5: for normalization, equivalent volumes were loaded on SDS-PAGE. Lanes 6–7, 2.5  $\mu$ g of purified protein. Lanes 8–9, 7  $\mu$ g of purified protein.

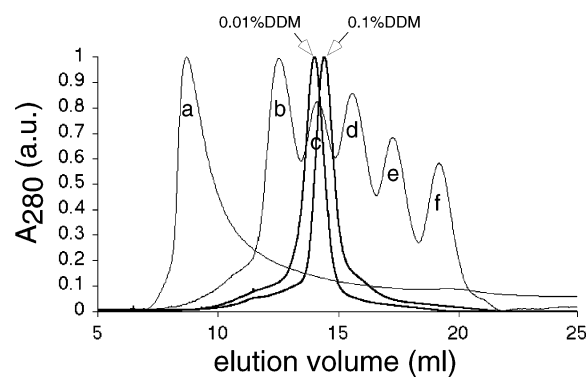


FIGURE 2: Analysis of purified MdfA by SE-HPLC. A typical elution profile ( $A_{280}$ ) of purified MdfA in 0.01% DDM or 0.1% DDM. Molecular mass markers (thin lines) are as follows: a, dextran blue, void volume marker; b, glutamate dehydrogenase, 290 kDa; c, lactate dehydrogenase, 142 kDa; d, enolase, 67 kDa; e, myokinase, 32 kDa; and f, cytochrome c, 12.4 kDa.

both in 0.01% and 0.1% DDM (Figure 2). Interestingly, the elution retention time for MdfA is dependent on the DDM concentration and corresponds to a molecular mass of  $\sim 146$  kDa at 0.01% DDM and  $\sim 112$  kDa at 0.1% DDM. Both particles are several-fold larger than the size expected from the calculated molecular mass of MdfA ( $\sim 45.5$  kDa, including a 6-histidine tag). These results suggest that MdfA is either oligomeric and/or associated with lipids and detergent molecules.

**Characterization of the DDM Content of Purified MdfA.** The DDM concentration in fractions collected during SE-HPLC experiments was determined as described in Experimental Procedures. When superimposed on the SE-HPLC elution profiles, the DDM maxima coincide with the MdfA peaks, indicating that MdfA is indeed loaded with DDM molecules (Figure 3A). As expected, MdfA-unbound DDM micelles have a longer retention time and, therefore, elute late during chromatography (Figure 3B). In order to quantify how many molecules of DDM are, on average, associated with each MdfA molecule, the amount of MdfA in the peak fractions was determined by total amino acid analysis (see Experimental Procedures). The results show a molar ratio of 1:165 (MdfA/DDM) in the 0.01% DDM preparation and 1:101 for MdfA purified in 0.1% DDM. These results are in general agreement with the size of the MdfA particles, as

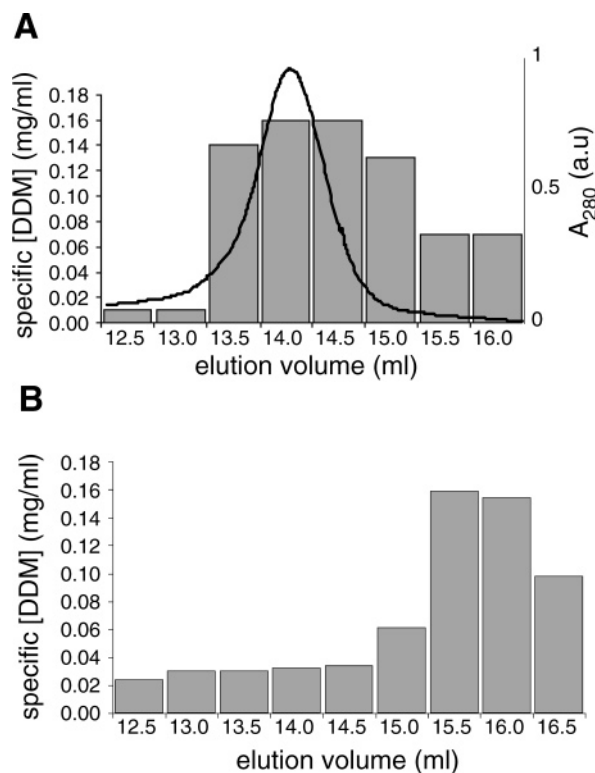


FIGURE 3: (A) Analysis of MdfA-associated DDM by SE-HPLC. DDM concentration in the MdfA elution fractions (bars) was determined as described, and shown in the context of the elution profile of MdfA ( $A_{280}$ , solid line). DDM concentration in the protein sample and the elution buffer is 0.01%. (B) Analysis of DDM micelles by SE-HPLC. A DDM sample without protein was subjected to all the same purification steps to which the sample in panel A was subjected. The sample was concentrated using a 30 kD-Vivaspin filter and subjected to SE-HPLC. Fractions were analyzed for DDM content as described.

Table 1: Characterization of Purified MdfA<sup>a</sup>

DDM concentration	0.01%	0.1%
purification yield (mg/10 L culture)	2.7 ± 0.3	3.0 ± 0.3
DDM/MdfA (w/w)	1.8 ± 0.1	1.1 ± 0.2
DDM/MdfA (mol/mol)	165 ± 9	101 ± 16
PL/MdfA (w/w)	0.43 ± 0.02	0.22 ± 0.05
PL/MdfA (mol/mol)	28 ± 1	13 ± 3
molecular mass (kDa)	147 ± 5	106 ± 10
MW <sub>SE-HPLC</sub> (kDa)	146 ± 2	112 ± 6

<sup>a</sup> The content of DDM, PLs, and MdfA in the sample was determined as described in Experimental Procedures. Weight/weight (w/w) and mol/mol ratios of DDM and PLs to MdfA in purified protein were then calculated. The molecular mass of the purified protein was calculated on the basis of molar ratios of MdfA, DDM, and PLs. Average molecular mass values of 0.7 kDa for *E. coli* PLs and 0.5 kDa for DDM were used in all calculations. The experimental molecular weight of purified protein (MW<sub>SE-HPLC</sub>) was determined using calibrated SE-HPLC (Figure 2). The entire characterization was performed at least three times.

observed in SE-HPLC (Table 1). Surprisingly, unlike our predictions, less DDM was found bound to MdfA when purified at high DDM concentrations.

**Characterization of the PL Content of Purified MdfA.** In addition to detergent molecules, purified membrane proteins are often associated with tightly bound lipid molecules. Because PLs represent the majority of lipids in the *E. coli* membranes (34), we determined PL concentrations in the purified MdfA preparations at 0.01% and 0.1% DDM (see

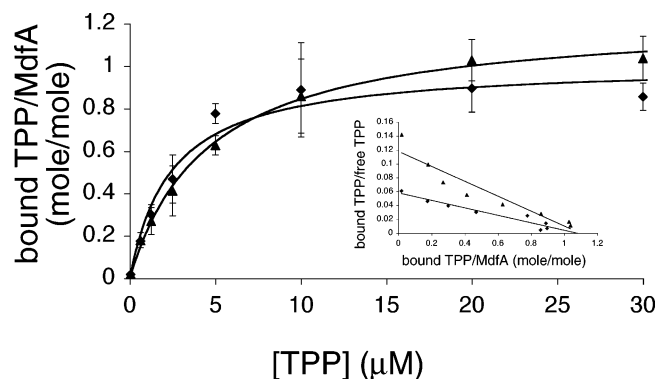


FIGURE 4: Purified MdfA is active in either 0.01% or 0.1% DDM. Specific TPP<sup>+</sup> binding by purified MdfA was measured as described (rhombus, 0.01% DDM, ~32 pmol of MdfA/measurement; triangle, 0.1% DDM, ~64 pmol of MdfA/measurement). The nonspecific component of binding to the resin alone was subtracted. The experiments were performed in triplicate, and the error bars indicate the standard deviation. Inset, Scatchard plot representation. The linear regression  $R^2$  is 0.929 for 0.01% DDM (rhombus) and 0.896 for 0.1% DDM (triangle).

Experimental Procedures). As detailed (Table 1), the results show that substantially fewer PLs are associated with MdfA prepared in 0.1% DDM (1:13 mol MdfA/mol PLs) compared to the amount PLs in MdfA prepared in 0.01% (1:28). Unlike the unexpected difference between the amounts of associated DDM, the difference in the amount of bound PLs is not surprising and suggests that more PLs are washed off MdfA during the purification protocol at high DDM concentrations.

**Determination of the Oligomeric Structure of MdfA in the Detergent Solution.** At low DDM concentration (0.01%), our studies show that on average, each molecule of MdfA is associated with approximately 165 DDM and 28 PL molecules. When combined, these molar ratios yield a total mass for the solubilized MdfA of  $147 \pm 5$  kDa. This molecular weight is in agreement with the calculated molecular mass of the MdfA particle obtained by SE-HPLC (Table 1, ~146 kDa), suggesting that MdfA is a monomer in DDM solution. When purified at a higher concentration of DDM (0.1%), each molecule of MdfA is associated with approximately 101 DDM and 13 PL molecules, leading to a total mass of ~106 kDa. In agreement with this value, the SE-HPLC yielded an MdfA particle that is smaller than the particle obtained at 0.01% DDM (Table 1, ~112 kDa). Therefore, we conclude that MdfA is monomeric in DDM solution regardless of the DDM concentration used for purification (see Discussion).

**Functional Characterization of Purified MdfA.** In order to compare the activity of MdfA purified under low and high DDM concentrations, we utilized a direct substrate-binding assay with radiolabeled TPP<sup>+</sup> as described previously (25). Briefly, MdfA was purified by metal affinity chromatography (single step) using 0.01% or 0.1% DDM in the purification buffers. After a dialysis step needed for the removal of imidazole, MdfA was re-immobilized by the resin, and tested for equilibrium TPP<sup>+</sup>-binding activity in the presence of the respective DDM concentrations used for purification. The results clearly show that regardless of the DDM concentration, MdfA specifically binds TPP<sup>+</sup> with a  $K_D$  of approximately 2.9 μM, and the stoichiometry of TPP<sup>+</sup>/MdfA is ~1:1 (Figure 4). These results suggest that MdfA retains its functional conformation even if the molar amounts of

associated DDM and PL molecules are as low as 101 and 13, respectively.

**Formation of 2D Crystals.** In order to characterize the oligomeric state of MdfA in the membrane and gain structural insight regarding the overall architecture of the transporter, we have crystallized MdfA in two dimensions. During an initial search for crystallization conditions, several parameters had paramount influence on crystal formation. The most important variables were temperature, lipid to protein ratio, lipid type, and the rate of detergent removal. Interestingly, the absolute concentrations of protein and lipids were less influential as long as an appropriate ratio was kept between them.

Initially, in order to expedite detergent removal, all crystallization trials were conducted at 25–30 °C. Under various conditions, ordered crystalline patches were formed (Figure 5A and B). Further analysis of these crystals using freeze-fracture techniques revealed that indeed the crystals are composed of protein molecules (Figure 5C). Unfortunately, Fourier transformation and freeze-fracture analysis both indicated that the crystals were multilayered and thus not amenable to analysis by electron microscopy (Figure 5B inset, Figure 5C, and Figure 5C inset). These problems were solved by lowering the dialysis temperature. As shown in Figure 6A, small, single layer crystalline patches were observed when crystallization was conducted at 14.5 °C. In order to compensate for the slower rate of detergent removal at this temperature, detergent absorbing beads were added to the dialysis buffer. The use of detergent absorbing beads led to an increase in size and order of crystals. Further optimization of the crystallization conditions yielded ordered crystals of adequate size (Figure 6B and C). The most ordered largest crystalline patches were produced by mixing a 1 mg/mL solution of purified MdfA in 0.1% *n*-dodecyl- $\beta$ -D-maltopyranoside with a 4 mg/mL solution of *E. coli* polar lipids (in 1% *n*-decyl- $\beta$ -D-maltopyranoside, (DM)) to a final lipid to protein ratio of 0.35 (w/w). Dialysis was conducted for 10–12 days at 14.5 °C against a 2000-fold volume excess of 20 mM NaOAc, 120 mM NaCl, 3 mM NaN<sub>3</sub>, 5 mM  $\beta$ -mercaptoethanol at pH 6, and 40 mg/mL Bio-beads.

**Projection Structure of MdfA.** Fourier transformations of images of negatively stained crystals revealed order up to 15 Å resolution (Figure 6C). Subsequent unbending and refinement of the images using the MRC program package (31) revealed reliable information up to 12 Å resolution (Figure 7A). Three space groups were identified to have comparable phase residuals by the program ALLSPACE:  $P2_12_12$ ,  $P4$ , and  $P42_12_1$ . The absence of certain symmetry related reflections in the calculated Fourier transforms allowed us to reject  $P4$  symmetry. Although the ALLSPACE residuals do not allow for differentiation between  $P2_12_12$  and  $P42_12_1$ , simple symmetry arguments favor  $P2_12_12$  over  $P42_12_1$  because the latter space group would require crystallographic 2-fold symmetry within the molecule, which is not biologically meaningful. As such, we have processed the images according to  $P2_12_12$  symmetry. Figure 7B shows the  $P2_12_12$  projection map of MdfA calculated from merging the eight best images. The square unit cell is  $a = 134.2$  Å (SD = 0.8,  $n = 8$ ),  $b = 133.9$  Å (SD = 0.61,  $n = 8$ ),  $g = 89.9^\circ$  (SD = 0.3,  $n = 8$ ), and contains four protein molecules. The MdfA monomer has an asymmetric envelope, roughly elliptical in shape, and is 55 Å in length along the long axis of the

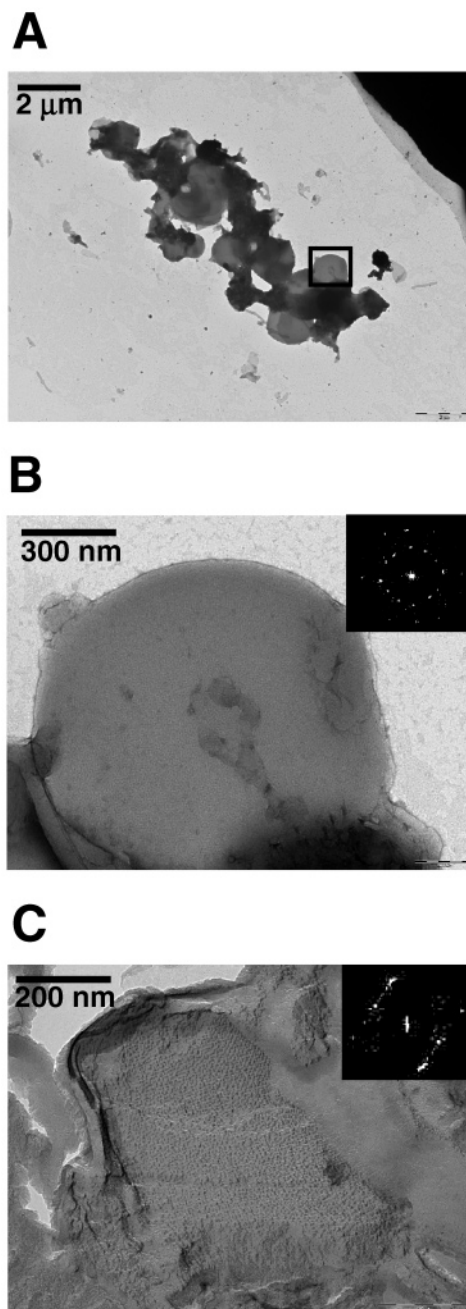


FIGURE 5: Electron microscope images of negatively stained crystals of MdfA obtained at 30 °C. (A) Low magnification overview of crystalline patches. (B) High magnification of the area boxed in A. Inset, FFT of the image. (C) Freeze fracture image of a similar sample. Inset, FFT of the image.

monomer. In projection, the width of the monomer varies between 23 and 43 Å. The surface area of the MdfA monomer is 1614 Å<sup>2</sup>, which according to the estimate of 140 Å<sup>2</sup> per TM (35, 36) corresponds to the presence of 12 TMs in MdfA. This surface area conforms well to those observed in projection maps of other secondary transporters (NhaA, 1824 Å<sup>2</sup> (37); OxIT, 1536 Å<sup>2</sup> (38); and MelB, 1813 Å<sup>2</sup> (39)). Although the present resolution offers little structural details, the structure provides information about the overall architecture of the transporter. The outer molecular envelope of MdfA most closely resembles that of OxIT (Figure 4 in (38)). However, unlike the quasi, 2-fold symmetry observed in OxIT, GlpT, and LacY (38, 40, 41), the densities observed in the projection map of MdfA are

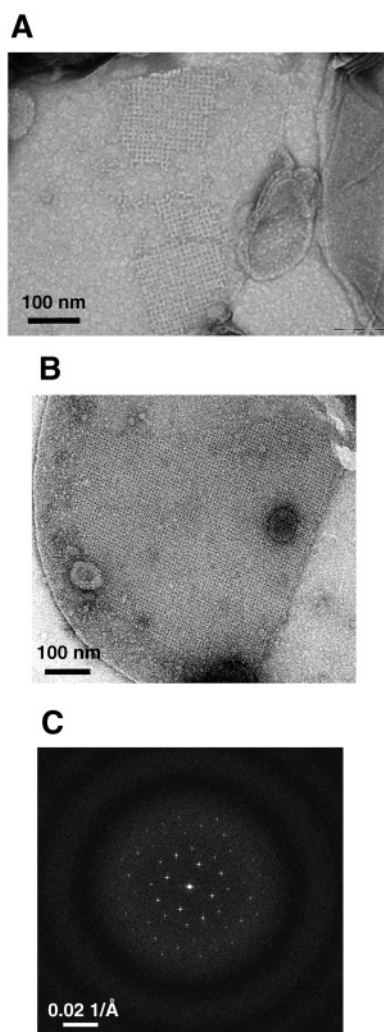


FIGURE 6: Electron microscope images of negatively stained 2D crystals of MdfA obtained at 14.5 °C. (A) Small patches of single layered crystals. (B) Addition of detergent absorbing beads and optimization of crystallization conditions lead to the formation of continuous crystalline patches. (C) FFT of the image shown in B.

distributed in an asymmetric manner. This asymmetry is not as pronounced as that observed in the projection maps of NhaA or MelB, but it may suggest that the helical packing of MdfA is slightly different from that of OxIT, GlpT, or LacY (*vide infra*). No continuous area of low density (suggesting the location of a translocation pore) is visible within the MdfA monomer (see Discussion).

A dimeric association of MdfA monomers can be observed in the projection map (Figure 7B and C). However, the contact between two MdfA monomers is restricted to a rather narrow region, approximately 10–20 Å wide. This limited contact between the monomers questions the functional significance of such an association and is most likely a result of crystal packing.

*Three-Dimensional Reconstruction of MdfA.* Next we reconstructed a 3D model of MdfA from a series of tilted images of negatively stained crystals. This approach has been successfully used in the past for other transporters and channels (42). Forty-three images were recorded at tilt angles ranging from  $\pm 15^\circ$  to  $\pm 45^\circ$ , and tilt geometries were manually calculated and later verified by the program EMTILT. The low angle tilts were then merged to the projection data set and subsequently to the higher tilts to

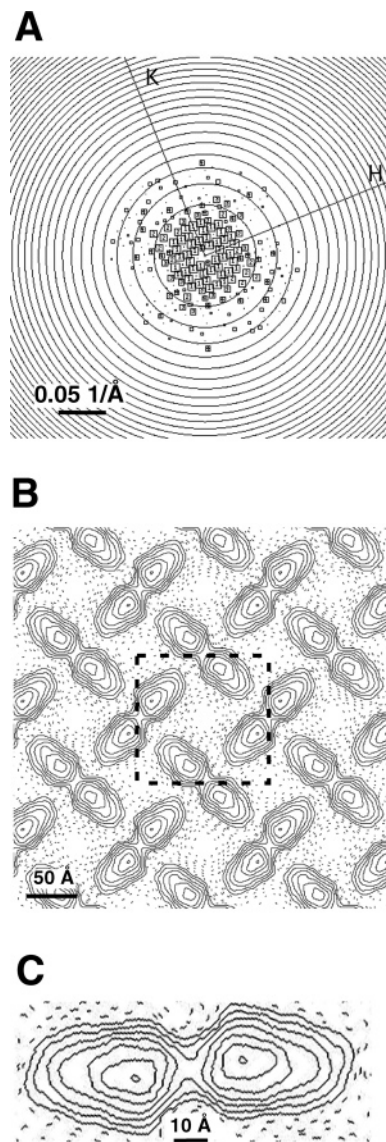


FIGURE 7: Analysis of 2D crystals of MdfA. (A) Image quality plot (IQ) of a single crystal. Each spot in the transform is represented by a square and an IQ number indicating the signal-to-noise ratio. Larger boxes and smaller IQ values reflect higher quality spots. (B)  $P2_12_12$  projection map of MdfA calculated from merging the eight best images. One unit cell is shown in the dashed box. (C) Close-up of an MdfA dimer taken from B.

produce the 3D data set. Interpolated fits to the experimental structure factors were calculated using the program LAT-LINE. The overall phase residual for the 3D map was  $18.7^\circ$  ( $90^\circ$  phase residual expected from random data) for 1983 reflections of image quality factor (IQ) values of 4 or better. A summary of the crystallographic data quality and image-processing parameters are shown in Table 2. A side view (parallel to the membrane plane) of the reconstructed 3D model of MdfA shows a heart shaped molecule that can roughly be divided into left and right domains (Figure 8). The pseudo 2-fold internal symmetry observed in OxIT, GlpT, and LacY is absent in MdfA, as was also suggested by the projection map. Another evident feature is the compactness of the structure relative to the more open structures displayed by both LacY and GlpT. Such compact conformation might represent an intermediate state, as was proposed for EmrD (43), between the two rocker switch conformations in the postulated alternating access mechanism

Table 2: Electron Crystallographic Image Statistics

two-sided plane group symmetry	$P2_12_12$
unit cell parameters	
<i>a</i> (Å)	$134.2 \pm 0.8$
<i>b</i> (Å)	$133.9 \pm 0.61$
$\gamma$ (deg)	$89.9 \pm 0.3$
no. of crystals used for the generation of the projection map	8
no. of crystals used in 3D reconstruction	43
range of defocus (Å)	5000–25000
no. of observations, $IQ \leq 4$	1317
no. of unique observations	754
overall phase residual to 15 Å (deg), $IQ \leq 5$	18.7

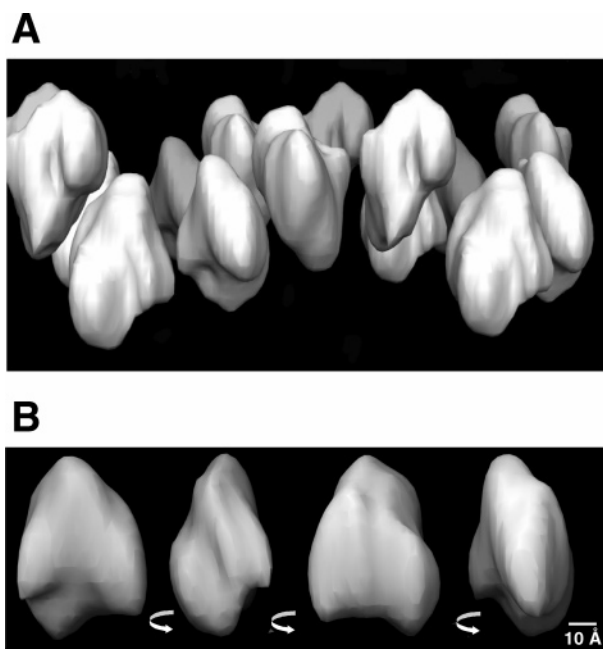


FIGURE 8: Three-dimensional reconstruction of MdfA. (A) Packing of MdfA dimers in three dimensions. The view is along the Y-axis. (B) Side views of a single MdfA monomer. The snapshots are rotated by 90° relative to one another.

of transport by GlpT and LacY (40, 41). This architecture might also represent a closed conformation of the transporter with an occluded substrate. However, both the resolution of the 2D structure presented here and the crystal structure of EmrD (3.5 Å) are not sufficient for the detection of a substrate molecule.

## DISCUSSION

We have investigated the properties of the secondary multidrug transporter MdfA by biochemical and structural means and demonstrated that the functional transporter is monomeric in a detergent solution and probably also in reconstituted proteoliposomes.

For biochemical studies, MdfA<sub>6HIS</sub> was purified by metal affinity chromatography using two different concentrations of detergent, close to its critical micellar concentration (CMC) and 10-fold higher (0.01% and 0.1% DDM, respectively). SE-HPLC analysis of the purified proteins and measurements of the amount of DDM and PLs bound to MdfA revealed that under both conditions, MdfA migrates as a monomer. Interestingly, however, the results also showed that MdfA binds less DDM under high DDM concentrations. Whereas the amount of bound PLs is usually inversely related

to the detergent concentration used during the purification (44, 45), it was unexpected that DDM exhibits a similar tendency. Although other explanations for this phenomenon cannot be excluded, we favor the possibility that a large amount of DDM is apparently associated with MdfA through bound PLs. Thus, when purified in high DDM concentrations, some of the DDM molecules replace MdfA-bound PL molecules, whereas others only remove PLs from the protein and transfer them to the detergent micelles. Consequently, less DDM remains attached to MdfA under these conditions.

Studies with other polytopic membrane proteins have shown that the amount of DDM bound to each protein molecule varies in the range of 105–290 molecules (26, 46–48), possibly dependent, among other factors, on the detergent used and its concentration. Thus, the amount of DDM bound to MdfA is consistent with these previously reported values. Similarly, the amount of PLs associated with MdfA is consistent with that of various purified polytopic membrane proteins (26, 44, 45).

Importantly, purified MdfA is active, as shown by equilibrium TPP<sup>+</sup>-binding assays, and binds the substrate with 1:1 stoichiometry, regardless of the DDM concentration used for purification. These results suggest that the amount of PLs bound to MdfA purified in 0.1% DDM is sufficient to maintain full equilibrium substrate-binding capacity. Whether the kinetics of association and dissociation of substrates from MdfA are more strictly dependent on the amount of bound PLs remains to be determined. In our previous work (25), the MdfA–TPP<sup>+</sup> binding stoichiometry was determined to be 0.6. This apparent contradiction with the present results can be reconciled by the fact that protein concentration was overestimated in the previous studies. Here, we have performed amino acid analysis in order to calibrate the various protein concentration assays and determine its absorbance coefficient at 280 nm. In conclusion, our present findings suggest that each molecule of MdfA binds one molecule of TPP<sup>+</sup>, lending support to the suggestion that MdfA is functional as a monomer.

To gain further insight into the oligomeric organization of MdfA in its natural environment, we have crystallized the transporter embedded in proteoliposomes. Electron crystallography of negatively stained 2D crystals have been successfully used in the past to obtain low-resolution structural information of transporters (42). Two-dimensional crystals of MdfA were formed in either membrane vesicles or membranous sheets, and the former proved to be more amenable to structural analysis by electron crystallography. The 15 Å projection map of MdfA (Figure 7) shows four protein molecules in each unit cell of the crystal lattice. Although two of these protein molecules are in close vicinity to one another, a closer look at the contact region between them reveals that it is quite narrow and thus questions the functional relevance of such an association. The surface area of each MdfA monomer (1614 Å<sup>2</sup>) conforms well with the presence of 12 TMs, as has also been suggested by extensive topological studies (20, 21). Similar surface areas with reminiscent molecular envelopes have been observed for other MFS transporters (LacY (41), GlpT (40), and OxlT (38)). It seems that regardless of the transported moiety, be it a sugar, glycerol-3-phosphate, oxalate, or hydrophobic drugs, some structural conservation persists within this superfamily (49). In contrast to the pseudo 2-fold internal

symmetry present in LacY, GlpT, or OxlT, the distribution of densities in MdfA lacks such symmetry. Such internal asymmetry may project the low sequence homology between the N'-terminal and C'-terminal halves of MdfA. No continuous area of low density can be defined in the projection map of MdfA. The lack of such an opening may be the result of the low resolution of our map but may also reflect a closed conformation of MdfA. Such a closed conformation was also observed in the recently published structure of the putative MFS multidrug transporter EmrD (43). Despite its low resolution, the 3D reconstruction of MdfA sheds some light on both the oligomeric organization of the transporter and of its conformation. Along the z-axis of the crystal lattice (perpendicular to the membrane plane), contacts between neighboring monomers are limited to a very narrow area, suggesting that these contacts are a result of crystal packing.

## ACKNOWLEDGMENT

We thank Werner Kuhlbrandt and Thomas Walz for their help and advice in the initial stages of the 2D crystallization project, Daniel Tal for his help during the SE-HPLC studies, and Lubov Ginzburg for help in the phospholipid assays.

## REFERENCES

- Bolhuis, H., van Veen, H. W., Poolman, B., Driessen, A. J., and Konings, W. N. (1997) Mechanisms of multidrug transporters, *FEMS Microbiol. Rev.* **21**, 55–84.
- Putman, M., Van Veen, H. W., Degener, J. E., and Konings, W. N. (2000) Antibiotic resistance: era of the multidrug pump, *Mol. Microbiol.* **36**, 772–773.
- Edgar, R., and Bibi, E. (1997) MdfA, an *Escherichia coli* multidrug resistance protein with an extraordinarily broad spectrum of drug recognition, *J. Bacteriol.* **179**, 2274–2280.
- Jack, D. L., Storms, M. L., Tchieu, J. H., Paulsen, I. T., and Saier, M. H., Jr. (2000) A broad-specificity multidrug efflux pump requiring a pair of homologous SMR-type proteins, *J. Bacteriol.* **182**, 2311–2313.
- Lewis, K., Naroditskaya, V., Ferrante, A., and Fokina, I. (1994) Bacterial resistance to uncouplers, *J. Bioenerg. Biomembr.* **26**, 639–646.
- Zgurskaya, H. I., and Nikaido, H. (2000) Multidrug resistance mechanisms: drug efflux across two membranes, *Mol. Microbiol.* **37**, 219–225.
- Nikaido, H. (1994) Prevention of drug access to bacterial targets: permeability barriers and active efflux, *Science* **264**, 382–388.
- Paulsen, I. T. (2003) Multidrug efflux pumps and resistance: regulation and evolution, *Curr. Opin. Microbiol.* **6**, 446–451.
- Saier, M. H., Jr., and Paulsen, I. T. (2001) Phylogeny of multidrug transporters, *Semin. Cell Dev. Biol.* **12**, 205–213.
- Marger, M. D., and Saier, M. H., Jr. (1993) A major superfamily of transmembrane facilitators that catalyze uniport, symport and antiport, *Trends Biochem. Sci.* **18**, 13–20.
- Lewinson, O., Adler, J., Sigal, N., and Bibi, E. (2006) Promiscuity in multidrug recognition and transport: the bacterial MFS Mdr transporters, *Mol. Microbiol.* **61**, 277–284.
- Bibi, E., Adler, J., Lewinson, O., and Edgar, R. (2001) MdfA, an interesting model protein for studying multidrug transport, *J. Mol. Microbiol. Biotechnol.* **3**, 171–177.
- Sigal, N., Cohen-Karni, D., Siemion, S., and Bibi, E. (2006) MdfA from *E. coli*, a model protein for studying secondary multidrug transport, *J. Mol. Microbiol. Biotechnol.* **11**, 308–317.
- Jin, Q., Yuan, Z., Xu, J., Wang, Y., Shen, Y., Lu, W., Wang, J., Liu, H., Yang, J., Yang, F., Zhang, X., Zhang, J., Yang, G., Wu, H., Qu, D., Dong, J., Sun, L., Xue, Y., Zhao, A., Gao, Y., Zhu, J., Kan, B., Ding, K., Chen, S., Cheng, H., Yao, Z., He, B., Chen, R., Ma, D., Qiang, B., Wen, Y., Hou, Y., and Yu, J. (2002) Genome sequence of *Shigella flexneri* 2a: insights into pathogenicity through comparison with genomes of *Escherichia coli* K12 and O157, *Nucleic Acids Res.* **30**, 4432–4441.
- Parkhill, J., Dougan, G., James, K. D., Thomson, N. R., Pickard, D., Wain, J., Churcher, C., Mungall, K. L., Bentley, S. D., Holden, M. T., Sebahia, M., Baker, S., Basham, D., Brooks, K., Chillingworth, T., Connerton, P., Cronin, A., Davis, P., Davies, R. M., Dowd, L., White, N., Farrar, J., Feltwell, T., Hamlin, N., Haque, A., Hien, T. T., Holroyd, S., Jagels, K., Krogh, A., Larsen, T. S., Leather, S., Moule, S., O'Gaora, P., Parry, C., Quail, M., Rutherford, K., Simmonds, M., Skelton, J., Stevens, K., Whitehead, S., and Barrell, B. G. (2001) Complete genome sequence of a multiple drug resistant *Salmonella enterica* serovar Typhi CT18, *Nature* **413**, 848–852.
- Parkhill, J., Wren, B. W., Thomson, N. R., Titball, R. W., Holden, M. T., Prentice, M. B., Sebahia, M., James, K. D., Churcher, C., Mungall, K. L., Baker, S., Basham, D., Bentley, S. D., Brooks, K., Cerdeno-Tarraga, A. M., Chillingworth, T., Cronin, A., Davies, R. M., Davis, P., Dougan, G., Feltwell, T., Hamlin, N., Holroyd, S., Jagels, K., Karlyshev, A. V., Leather, S., Moule, S., Oyston, P. C., Quail, M., Rutherford, K., Simmonds, M., Skelton, J., Stevens, K., Whitehead, S., and Barrell, B. G. (2001) Genome sequence of *Yersinia pestis*, the causative agent of plague, *Nature* **413**, 523–527.
- Lewinson, O., Adler, J., Poelarends, G. J., Mazurkiewicz, P., Driessen, A. J., and Bibi, E. (2003) The *Escherichia coli* multidrug transporter MdfA catalyzes both electrogenic and electroneutral transport reactions, *Proc. Natl. Acad. Sci. U.S.A.* **100**, 1667–1672.
- Mine, T., Morita, Y., Kataoka, A., Mizushima, T., and Tsuchiya, T. (1998) Evidence for chloramphenicol/H<sup>+</sup> antiport in Cmr (MdfA) system of *Escherichia coli* and properties of the antiporter, *J. Biochem. (Tokyo)* **124**, 187–193.
- Lewinson, O., Padan, E., and Bibi, E. (2004) Alkalitolerance: a biological function for a multidrug transporter in pH homeostasis, *Proc. Natl. Acad. Sci. U.S.A.* **101**, 14073–14078.
- Adler, J., and Bibi, E. (2002) Membrane topology of the multidrug transporter MdfA: complementary gene fusion studies reveal a nonessential C-terminal domain, *J. Bacteriol.* **184**, 3313–3320.
- Edgar, R., and Bibi, E. (1999) A single membrane-embedded negative charge is critical for recognizing positively charged drugs by the *Escherichia coli* multidrug resistance protein MdfA, *EMBO J.* **18**, 822–832.
- Adler, J., and Bibi, E. (2004) Determinants of substrate recognition by the *Escherichia coli* multidrug transporter MdfA identified on both sides of the membrane, *J. Biol. Chem.* **279**, 8957–8965.
- Adler, J., and Bibi, E. (2005) Promiscuity in the geometry of electrostatic interactions between the *Escherichia coli* multidrug resistance transporter MdfA and cationic substrates, *J. Biol. Chem.* **280**, 2721–2729.
- Sigal, N., Vardy, E., Molshanski-Mor, S., Eitan, A., Pilpel, Y., Schuldiner, S., and Bibi, E. (2005) 3D model of the *Escherichia coli* multidrug transporter MdfA reveals an essential membrane-embedded positive charge, *Biochemistry* **44**, 14870–14880.
- Lewinson, O., and Bibi, E. (2001) Evidence for simultaneous binding of dissimilar substrates by the *Escherichia coli* multidrug transporter MdfA, *Biochemistry* **40**, 12612–12618.
- Butler, P. J., Ubarretxena-Belandia, I., Warne, T., and Tate, C. G. (2004) The *Escherichia coli* multidrug transporter EmrE is a dimer in the detergent-solubilised state, *J. Mol. Biol.* **340**, 797–808.
- Jap, B. K., Zulauf, M., Scheybani, T., Hefli, A., Baumeister, W., Aebi, U., and Engel, A. (1992) 2D crystallization: from art to science, *Ultramicroscopy* **46**, 45–84.
- Kuhlbrandt, W. (1992) Two-dimensional crystallization of membrane proteins, *Q. Rev. Biophys.* **25**, 1–49.
- Levy, D., Mosser, G., Lambert, O., Moeck, G. S., Bald, D., and Rigaud, J. L. (1999) Two-dimensional crystallization on lipid layer: A successful approach for membrane proteins, *J. Struct. Biol.* **127**, 44–52.
- Walz, T., and Grigorieff, N. (1998) Electron crystallography of two-dimensional crystals of membrane proteins, *J. Struct. Biol.* **121**, 142–161.
- Crowther, R. A., Henderson, R., and Smith, J. M. (1996) MRC image processing programs, *J. Struct. Biol.* **116**, 9–16.
- Agard, D. A. (1983) A least-squares method for determining structure factors in three-dimensional tilted-view reconstructions, *J. Mol. Biol.* **167**, 849–852.
- Adler, J., Lewinson, O., and Bibi, E. (2004) Role of a conserved membrane-embedded acidic residue in the multidrug transporter MdfA, *Biochemistry* **43**, 518–525.
- Raetz, C. R., and Dowhan, W. (1990) Biosynthesis and function of phospholipids in *Escherichia coli*, *J. Biol. Chem.* **265**, 1235–1238.

35. Eskandari, S., Wright, E. M., Kreman, M., Starace, D. M., and Zampighi, G. A. (1998) Structural analysis of cloned plasma membrane proteins by freeze-fracture electron microscopy, *Proc. Natl. Acad. Sci. U.S.A.* *95*, 11235–11240.
36. Conroy, M. J., Jamieson, S. J., Blakey, D., Kaufmann, T., Engel, A., Fotiadis, D., Merrick, M., and Bullough, P. A. (2004) Electron and atomic force microscopy of the trimeric ammonium transporter AmtB, *EMBO Rep.* *5*, 1153–1158.
37. Williams, K. A., Geldmacher-Kaufner, U., Padan, E., Schuldiner, S., and Kuhlbrandt, W. (1999) Projection structure of NhaA, a secondary transporter from *Escherichia coli*, at 4.0 Å resolution, *EMBO J.* *18*, 3558–3563.
38. Heymann, J. A., Sarker, R., Hirai, T., Shi, D., Milne, J. L., Maloney, P. C., and Subramaniam, S. (2001) Projection structure and molecular architecture of OxlT, a bacterial membrane transporter, *EMBO J.* *20*, 4408–4413.
39. Hacksell, I., Rigaud, J. L., Purhonen, P., Pourcher, T., Hebert, H., and Leblanc, G. (2002) Projection structure at 8 Å resolution of the melibiose permease, an Na-sugar co-transporter from *Escherichia coli*, *EMBO J.* *21*, 3569–3574.
40. Huang, Y., Lemieux, M. J., Song, J., Auer, M., and Wang, D. N. (2003) Structure and mechanism of the glycerol-3-phosphate transporter from *Escherichia coli*, *Science* *301*, 616–620.
41. Abramson, J., Smirnova, I., Kasho, V., Verner, G., Kaback, H. R., and Iwata, S. (2003) Structure and mechanism of the lactose permease of *Escherichia coli*, *Science* *301*, 610–615.
42. Rosenberg, M. F., Kamis, A. B., Aleksandrov, L. A., Ford, R. C., and Riordan, J. R. (2004) Purification and crystallization of the cystic fibrosis transmembrane conductance regulator (CFTR), *J. Biol. Chem.* *279*, 39051–39057.
43. Yin, Y., He, X., Szewczyk, P., Nguyen, T., and Chang, G. (2006) Structure of the multidrug transporter EmrD from *Escherichia coli*, *Science* *312*, 741–744.
44. Lemieux, M. J., Song, J., Kim, M. J., Huang, Y., Villa, A., Auer, M., Li, X. D., and Wang, D. N. (2003) Three-dimensional crystallization of the *Escherichia coli* glycerol-3-phosphate transporter: a member of the major facilitator superfamily, *Protein Sci.* *12*, 2748–2756.
45. Guan, L., Smirnova, I. N., Verner, G., Nagamori, S., and Kaback, H. R. (2006) Manipulating phospholipids for crystallization of a membrane transport protein, *Proc. Natl. Acad. Sci. U.S.A.* *103*, 1723–1726.
46. Heuberger, E. H., Veenhoff, L. M., Durkens, R. H., Friesen, R. H., and Poolman, B. (2002) Oligomeric state of membrane transport proteins analyzed with blue native electrophoresis and analytical ultracentrifugation, *J. Mol. Biol.* *317*, 591–600.
47. Kaufmann, T. C., Engel, A., and Remigy, H. W. (2006) A novel method for detergent concentration determination, *Biophys. J.* *90*, 310–317.
48. Ravaut, S., Do Cao, M. A., Jidenko, M., Ebel, C., Le Maire, M., Jault, J. M., Di Pietro, A., Haser, R., and Aghajari, N. (2006) The ABC transporter BmrA from *Bacillus subtilis* is a functional dimer when in a detergent-solubilized state, *Biochem. J.* *395*, 345–353.
49. Vardy, E., Arkin, I. T., Gottschalk, K. E., Kaback, H. R., and Schuldiner, S. (2004) Structural conservation in the major facilitator superfamily as revealed by comparative modeling, *Protein Sci.* *13*, 1832–1840.

BI602405W